



Published in final edited form as:

Hepatology. 2012 June ; 55(6): 1711–1721. doi:10.1002/hep.25559.

Hedgehog Pathway Activation Parallels Histologic Severity of Injury and Fibrosis in Human Nonalcoholic Fatty Liver Disease

Cynthia D. Guy¹, Ayako Suzuki², Marzena Zdanowicz², Manal F. Abdelmalek², James Burchette¹, Aynur Unalp³, and Anna Mae Diehl² for the NASH CRN

¹Department of Pathology, Duke University Medical Center, Durham, NC

²Division of Gastroenterology and Hepatology, Department of Medicine, Duke University Medical Center, Durham, NC

³Johns Hopkins Center for Clinical Trials, Baltimore, MD

Abstract

The Hedgehog (Hh) signaling pathway mediates several processes that are deregulated in patients with the metabolic syndrome (e.g., fat mass regulation, vascular/endothelial remodeling, liver injury and repair, and carcinogenesis). The severity of nonalcoholic fatty liver disease (NAFLD) and the metabolic syndrome generally correlate. Therefore, we hypothesized that the level of Hh pathway activation would increase in parallel with the severity of liver damage in NAFLD. To assess potential correlations between known histologic and clinical predictors of advanced liver disease and Hh pathway activation, immunohistochemistry was performed on liver biopsies from a large well-characterized cohort of NAFLD patients (n=90) enrolled in the Nonalcoholic Steatohepatitis Clinical Research Network (NASH CRN) Database 1 study. Increased Hh activity (evidenced by accumulation of Hh-ligand producing cells and Hh-responsive target cells) strongly correlated with portal inflammation, ballooning, and fibrosis stage (each $p < 0.0001$), supporting a relationship between Hh pathway activation and liver damage. Pathway activity also correlated significantly with markers of liver repair, including numbers of hepatic progenitors and myofibroblastic cells (both $p < 0.03$). In addition, various clinical parameters that have been linked to histologically-advanced NAFLD, including increased patient age ($p < 0.005$), BMI ($p < 0.002$), waist circumference ($p < 0.0007$), homeostatic model assessment of insulin resistance (HOMA-IR) ($p < 0.0001$) and hypertension ($p < 0.02$), correlated with hepatic Hh activity. **Conclusion:** In NAFLD patients, the level of hepatic Hh pathway activity is highly correlated with the severity of liver damage and with metabolic syndrome parameters that are known to be predictive of advanced liver disease. Hence, deregulation of the Hh signaling network may contribute to the pathogenesis and sequelae of liver damage that develops with the metabolic syndrome.

Keywords

Sonic hedgehog; nonalcoholic steatohepatitis; advanced fibrosis; metabolic syndrome

INTRODUCTION

Nonalcoholic fatty liver disease (NAFLD) is strongly associated with obesity. Because of the current obesity epidemic, NAFLD is now one of the most prevalent liver diseases in the world and a major cause of cirrhosis and liver-related mortality [1]. Fortunately, only some of the many individuals with NAFLD will ever develop progressive liver injury that results in steatohepatitis (SH), cirrhosis, or primary liver cancer. Therefore, efficient and accurate identification of patients who are most likely to develop progressive liver damage is crucial

so that such individuals can be targeted for more aggressive surveillance and therapeutic

Corresponding Author: Anna Mae Diehl, MD Chief, Division of Gastroenterology and Hepatology, Department of Medicine, Duke University, Synderman Building (GSRB-1), 595 LaSalle Street, Suite 1073, Durham, NC 27710, USA, Phone Number: 919-684-2616 Fax Number: 919-684-4183 annamae.diehl@duke.edu.

Members of the Nonalcoholic Steatohepatitis Clinical Research Network: *Clinical Centers*

Baylor College of Medicine, Houston, TX: Stephanie H. Abrams, MD, MS; Leanel Angeli Fairly, RN

Case Western Reserve University Clinical Centers:

• **MetroHealth Medical Center, Cleveland, OH:** Arthur J. McCullough, MD; Patricia Brandt; Diane Bringman, RN (2004-2008); Srinivasan Dasarathy, MD; Jaividhya Dasarathy, MD; Carol Hawkins, RN; Yao-Chang Liu, MD (2004-2009); Nicholette Rogers, PhD, PA-C (2004-2008); Margaret Stager, MD (2004-2009)

• **Cleveland Clinic Foundation, Cleveland, OH:** Arthur J. McCullough, MD; Srinivasan Dasarathy, MD; Mangesh Pagadala, MD; Ruth Sargent, LPN; Lisa Yerian, MD; Claudia Zein, MD

California Pacific Medical Center: Raphael Merriman, MD; Anthony Nguyen

Children's National Medical Center, Washington DC: Parvathi Mohan, MD; Kavita Nair

Cincinnati Children's Hospital Medical Center, Cincinnati, OH: Stephanie DeVore; Rohit Kohli, MD; Kathleen Lake; Stavra Xanthakos, MD

Duke University Medical Center, Durham, NC: Manal F. Abdelmalek, MD, MPH; Stephanie Buie; Anna Mae Diehl, MD; Marcia Gottfried, MD (2004-2008); Cynthia Guy, MD; Meryt Hanna; Paul Killenberg, MD (2004-2008); Samantha Kwan, MS (2006-2009); Yi-Ping Pan; Dawn Piercy, FNP; Melissa Smith

Indiana University School of Medicine, Indianapolis, IN: Elizabeth Byam, RN; Naga Chalasani, MD; Oscar W. Cummings, MD; Ann Klipsch, RN; Jean P. Molleston, MD; Linda Ragozzino, RN; Girish Subbarao, MD; Raj Vuppalachchi, MD

Johns Hopkins Hospital, Baltimore, MD: Kimberly Pfeifer, RN; Ann Scheimann, MD; Michael Torbenson, MD

Mount Sinai Kravis Children's Hospital: Nanda Kerkar, MD; Sreevidya Narayanappa; Frederick Suchy, MD

Northwestern University Feinberg School of Medicine/Children's Memorial Hospital: Mark H. Fishbein, MD; Katie Jacques; Ann Quinn, RD; Cindy Riazzi, RN; Peter F. Whittington, MD

Seattle Children's Hospital & Research Institute, WA: Melissa Coffey; Sarah Galdzicka, Karen Murray, MD; Melissa Young

Saint Louis University, St Louis, MO: Sarah Barlow, MD (2002-2007); Jose Derooy, MD; Joyce Hoffmann; Debra King, RN; Andrea Morris; Joan Siegner, RN; Susan Stewart, RN; Brent A. Neuschwander-Tetri, MD; Judy Thompson, RN

University of California San Diego, San Diego, CA: Cynthia Behling, MD, PhD; Janis Durelle; Tarek Hassanein, MD (2004-2009); Joel E. Lavine, MD, PhD; Rohit Loomba, MD; Anya Morgan; Steven Rose, MD (2007-2009); Heather Patton, MD; Jeffrey B. Schwimmer, MD; Claude Sirlin, MD; Tanya Stein, MD (2005-2009)

University of California San Francisco, San Francisco, CA: Bradley Aouizerat, PhD; Kiran Bambha, MD (2006-2010); Nathan M. Bass, MD, PhD; Linda D. Ferrell, MD; Danuta Filipowski, MD; Bo Gu (2009-2010); Raphael Merriman, MD (2002-2007); Mark Pabst; Monique Rosenthal (2005-2010); Philip Rosenthal, MD; Tessa Steel (2006-2008)

University of Washington Medical Center, Seattle, WA: Matthew Yeh, MD, PhD

Virginia Commonwealth University, Richmond, VA: Sherry Boyett, RN, BSN; Melissa J. Contos, MD; Michael Fuchs, MD; Amy Jones; Velimir AC Luketic, MD; Puneet Puri, MD; Bimaljit Sandhu, MD (2007-2009); Arun J. Sanyal, MD; Carol Sargeant, RN, BSN, MPH; Kimberly Noble; Melanie White, RN, BSN (2006-2009)

Virginia Mason Medical Center, Seattle, WA: Kris V. Kowdley, MD1; Jody Mooney, MS; James Nelson, PhD; Sarah Ackermann; Cheryl Saunders, MPH; Vy Trinh; Chia Wang, MD 1 original grant with University of Washington

Washington University, St. Louis, MO: Elizabeth M. Brunt, MD

Resource Centers

National Cancer Institute, Bethesda, MD: David E. Kleiner, MD, PhD

National Institute of Child Health and Human Development, Bethesda, MD: Gilman D. Grave, MD

National Institute of Diabetes and Digestive and Kidney Diseases, Bethesda, MD: Edward C. Doo, MD; Jay H. Hoofnagle, MD; Patricia R. Robuck, PhD, MPH (Project Scientist)

Johns Hopkins University, Bloomberg School of Public Health (Data Coordinating

Center), Baltimore, MD: Patricia Belt, BS; Frederick L. Brancati, MD, MHS (2003-2009); Jeanne M. Clark, MD, MPH; Ryan Colvin, MPH; Michele Donithan, MHS; Mika Green, MA; Rosemary Hollick (2003-2005); Milana Isaacson, BS; Wana Kim, BS; Alison Lydecker, MPH (2006-2008); Pamela Mann, MPH (2008-2009); Laura Miriel; Alice Sternberg, ScM; James Tonascia, PhD; Aynur Unalp-Arida, MD, PhD; Mark Van Natta, MHS; Ivana Vaughn, MPH; Laura Wilson, ScM; Katherine Yates, ScM

Conflict of Interest: The authors report no conflict of interest.

Author Contributions: Cynthia D Guy contributed to generation of research idea, interpretation of histologic data, analysis and interpretation of data, manuscript writing, and critical review of manuscript for final submission.

Ayako Suzuki contributed to statistical analysis, interpretation of data and drafting of the manuscript.

Marzena Zdanowicz optimized and performed most of the immunohistochemistry of liver biopsy slides, performed all the immunohistochemical evaluations, and contributed to data analyses.

Manal F. Abdelmalek contributed to data acquisition, interpretation of data and critical revision of the manuscript for important intellectual content.

James Burchette optimized and performed some of the immunohistochemistry of liver biopsy slides and critical review of the manuscript for final submission.

Aynur Unalp-Arida contributed to data management, statistical analysis and critical revision of the manuscript.

Anna Mae Diehl contributed to generation of research idea, contributed to data acquisition, interpretation of data, data analysis, manuscript writing, and critical review and revision of the manuscript for important intellectual content.

interventions to optimize the outcomes and minimize the costs of the NAFLD epidemic. Success has been stymied by our relatively poor understanding of the processes that regulate the outcomes of fatty liver injury.

Research involving experimental animals is often used to delineate key mechanisms and pilot therapies for human diseases with long and/or seemingly-idiosyncratic natural histories. In NAFLD, however, this approach has been hampered by the lack of small animal models of steatohepatitis and progressive liver fibrosis that also mimic the typical metabolic perturbations of human NAFLD [2]. None-the-less, recent studies in mice demonstrated that the development of SH and fibrosis correlated strongly with the intensity and duration of Hedgehog (Hh) pathway activation that developed during fatty liver injury [3]. Other work in cultured cells demonstrated that Hh ligands stimulate quiescent hepatic stellate cells to become myofibroblastic, promote proliferation of liver myofibroblasts and progenitors, inhibit apoptosis of these cell types, and up-regulate production of chemokines for various types of immune cells [4, 5]. Therefore, it is conceivable that inter-individual differences in Hh pathway activity contribute to the variable outcomes of fatty liver injury in NAFLD patients. This concept was supported by immunohistochemical staining of liver biopsy samples from a small number of NAFLD patients [3]. The resultant data showed that the hepatic content of Hh ligand producing cells, as well as the burden of Hh-responsive liver cells, increased in parallel with fibrosis stage. However, the fact that the analysis was performed in only a small number of patients from a single institution raised valid concerns amongst clinicians who questioned whether the selected cohort was representative of the general NAFLD population. Further investigation of this issue is warranted and therefore, the objective of the present study was to evaluate the relationship between the level of Hh pathway activity and severity of liver inflammation and fibrosis in a large, representative cohort of NAFLD patients.

PATIENTS AND METHODS

Study Design and Population

We performed a cross-sectional analysis using data and liver sections from a representative subset (n=90) of all subjects in the Nonalcoholic Steatohepatitis Clinical Research Network (NASH CRN) Database 1 Study (n=1044) [6]. Liver histologic data were available for 864 of these 1044 subjects, but only 232 of those individuals fulfilled the following criteria: 1)

18 years of age, 2) no significant alcohol consumption (14 drinks/week in men or 7 drinks/week in women on average within the past 2 years) or other coexisting causes of chronic liver disease, 3) liver biopsy of 15 mm in length performed within 6 months of enrollment into the Database, 4) unstained tissue sections available for immunohistochemical staining, and 5) the corresponding H&E and Masson trichrome stained liver biopsy slides had already been scored by the NASH CRN Pathology Committee. Our study cohort (n=90) was comprised of the first 30 consecutive cases from each of the following three histologically-defined groups: 1) NAFL (simple steatosis/not definite NASH) with no-to-early fibrosis (stage 0, stage 1, or stage 2) (N= 87); 2) definite NASH with early fibrosis (N=73); and 3) NAFL or NASH with advanced fibrosis (stage 3 or stage 4) (N=72). Case selection was performed by the NASH CRN Data Coordinating Center. The NASH Clinical Research Network studies were approved by the Institutional Review Boards at each participating center.

Histologic Evaluation of NAFLD

Liver biopsies from all of the cases in the present study had been stained with hematoxylin-eosin and Masson's trichrome, reviewed and scored by the NASH CRN Pathology Committee according to the published NASH CRN scoring system [7]. Briefly, portal

inflammation was graded as 0 (none to minimal), 1 (mild), or 2 (greater than mild). Hepatocyte ballooning was graded as 0 (none), 1 (few), or 2 (many). Fibrosis was staged as 0 (no pathologic fibrosis), 1 (centrilobular or periportal pericellular fibrosis), 2 (centrilobular pericellular and periportal fibrosis), 3 (bridging fibrosis), or 4 (cirrhosis). In addition to data for portal inflammation, hepatocyte ballooning, and fibrosis, we analyzed the complete histologic data set from this cohort to determine if any other standard histopathological parameter(s) correlated with evidence of Hh pathway activity as revealed by immunostaining of banked liver sections from the same patients. Because no relationships were demonstrated between Hh immunostaining and levels of hepatic steatosis or lobular inflammation, the Results section details only the findings that were noted with regard to portal inflammation, hepatocyte ballooning, and liver fibrosis.

Immunohistochemical evaluations

Three unstained slides from each patient's formalin-fixed paraffin-embedded liver biopsy were used for immunohistochemistry (IHC) to assess production of Sonic hedgehog (Shh) ligand and accumulation of Hh-responsive cells (demonstrated by nuclear staining for the Hh-regulated transcription factor, Gli2). To further characterize the types of cells that were Hh-responsive, representative sections from each histologic subgroup were co-stained for Gli2 and keratin 7 (K7, a marker of liver progenitors), or Gli2 and vimentin (a marker of mesenchymal cells). Remaining sections were stained for α -SMA, a myofibroblast marker that correlates with fibrosis severity.

Details of the IHC methods and antibodies have been published [3, 5, 8]. Positive staining for Shh, vimentin, and α -SMA were semi-quantified using 10x objective low power fields (100x magnification) as a percentage of the total surface area and graded into 5 categories: grade 1 (less than 20%), grade 2 (20-39%), grade 3 (40-59%), grade 4 (60-79%) and grade 5 (80%). For the Gli2/K7 double stain, total number of K7+ cells, and K7+/gli2+ double-positive cells, were counted in five 40x objective high power fields (400x magnification) to determine the average number of positively-stained cells.

Clinical information

All clinical information was collected within 6 months of the liver biopsy. Age, body mass index (BMI, kg/m²), waist circumference (cm), homeostasis model assessment–insulin resistance (HOMA-IR), presence or absence of diabetes mellitus and hypertension were evaluated. Clinical characteristics are reported as the mean \pm SD for continuous variables or as a proportion with a condition for categorical variables.

Statistical analyses

To assess associations between the immunohistochemistry scores and the H&E and trichrome scores, we performed Wilcoxon rank sum tests or Kruskal-Wallis tests. For post-hoc comparison, Wilcoxon rank sum tests were used. To assess associations between the level of Hh pathway activity and known clinical risk factors for advanced fibrosis, we performed ordinal logistic regression or linear regression analyses, with and without adjusting for other factors. JMP statistical software version 7.0 (SAS institute Inc., Cary, NC) was used for analysis and differences considered to be statistically significant when the p-values were less than 0.05, except for the post-hoc comparison in which α -levels were adjusted by 0.05/numbers of pairs in a comparison.

RESULTS

Clinical and histologic characteristics of the study population

The clinical and histologic characteristics of the study population are summarized in Table 1. The mean age and BMI of the study population were 48 ± 13 years and 35 ± 7 kg/m². Women comprised 59% of the cohort, 30% had diabetes mellitus, 46% had hypertension, and 56% had hyperlipidemia. Forty three percent of our cohort had significant ballooning (grade 2) and 33% had advanced fibrosis (S3-4).

Sonic Hedgehog (Shh) expression correlates with severity of ballooning, portal inflammation, and fibrosis stage in NAFLD

In animal models of NAFLD, Hh pathway activation has been linked to fibrogenesis [3]. Therefore Shh immunohistochemistry was performed on liver sections from 84 patients with different stages of fibrosis (S0, n=21; S1, n=21; S2, n=14; S3, n=19; S4, n=9). Positive staining was semi-quantified (i.e., graded) as described in the Methods. In this relatively large cohort of NAFLD patients, the hepatic content of Shh-expressing cells increased with fibrosis stage (Fig 1a-d). Moreover, the relationship between the level of Shh expression and fibrosis severity was highly significant (Fig 1e, $p < 0.0001$).

Given that studies in animal models demonstrated that Hh ligands stimulate chemokine production by ductular cells and result in hepatic recruitment of certain types of immune cell [5,9], we examined the relationship between Shh expression and portal inflammation in these subjects. Portal inflammation was strongly associated with Shh expression ($p < 0.0001$); mean rank and SD of Shh expression in patients with grade 0, grade 1, and grade 2 portal inflammation were 1.7 ± 0.9 , 2.8 ± 1.3 , and 4.0 ± 1.0 , respectively. Shh expression in subjects with grade 1 portal inflammation was higher than in those with grade 0 portal inflammation ($p < 0.015$) and lower than in subjects with grade 2 portal inflammation ($p < 0.0001$) (adjusted α -level = 0.017).

Inflammatory mediators have been implicated in the pathogenesis of NASH and are known to provoke various types of cellular stress, including endoplasmic reticulum (ER) stress. Ballooned hepatocytes exhibit features of ER stress and treating mouse hepatocytes with tunicamycin to induce ER stress stimulated them to express Shh mRNA and protein [10]. Therefore, we next evaluated the relationship between hepatocyte ballooning and Shh expression. Ballooned hepatocytes stained strongly for Shh in this group of NAFLD patients (Fig 2a-c) and the level of Shh expression strongly correlated with the severity of hepatocyte ballooning (Fig 2d, $p < 0.0001$).

Numbers of Gli2 (+) cells increase with fibrosis stage, portal inflammation, and ballooning in NAFLD

Shh interacts with receptors on the surface of Hh-responsive target cells to trigger Hh signaling that results in the nuclear localization of the Hh-regulated transcription factor, Gli2 [11]. We stained liver sections from a representative subset of our NAFLD patients to assess the relationship between Shh production and accumulation of cells with nuclear Gli2 staining. As expected, there was a positive correlation between Shh expression and Gli2 expression in these subjects ($p < 0.0001$). To discern potential relationships between the level of Hh pathway activation (as evidenced by accumulation of Gli2-expressing cells) and various outcomes of liver injury, 39 cases with different stages of liver fibrosis were selected for analysis (S0, n = 5; S1, n=11; S2, n=7; S3, n=9; S4, n=7). Hepatic accumulation of Hh-responsive cells (i.e., gli2 positive cells) increased with fibrosis stage (Fig 3a-d) and was particularly robust in patients with advanced (S3 and S4) fibrosis (Fig 3e, $p < 0.0001$).

Portal inflammation is a potential consequence of Hh pathway activation [5] and has also been linked to fibrogenesis in NAFLD [9]. To discern potential relationships between the accumulation of Gli2-expressing cells and portal inflammation, the same 39 cases with different grades of portal inflammation (G0, n=2; G1, n=24; G2, n=13) were analyzed. Indeed, we found that the severity of portal inflammation was significantly positively associated with numbers of Gli2+ liver cells (Fig 3f, $p < 0.02$).

Ballooned hepatocytes produce Hh ligands [10]. Hence, we examined the relationship between hepatic accumulation of Gli2-expressing cells and the severity of hepatocyte ballooning in this group of NAFLD patients. A subset of cases with a range of ballooning scores (G0, n=7; G1, n=13; G2, n=19) were stained for Gli2. Although there was considerable overlap in hepatic accumulation of Gli2-expressing cells among subject with different grades of ballooning, ballooning and Gli2 expression were significantly associated ($p < 0.005$).

Hepatic accumulation of Hh-responsive liver progenitors and myofibroblastic cells parallels fibrosis stage in NAFLD

It has long been known that hepatic progenitors accumulate in parallel with the severity of liver myofibroblast accumulation and liver fibrosis in NAFLD [12]. This has prompted speculation that injury-related factors might arrest epithelial differentiation of liver progenitors, while promoting the outgrowth of myofibroblastic populations. Hh ligands generally maintain Hh-responsive epithelial-type progenitors in a relatively undifferentiated state, but promote the growth of Hh-responsive myofibroblastic cells [3, 13]. Therefore, we co-stained liver sections from 16 unique NAFLD patients to demonstrate cells that co-expressed Gli2 and K7, a marker of liver epithelial progenitors. Sections were analyzed from patients across the spectrum of fibrosis (S0, n=1; S1, n=5; S2, n=2; S3, n=5; S4, n=3). Consistent with published data, the total number of K7+ cells increased in advanced fibrosis ($p < 0.05$). Double staining for K7 and Gli2 demonstrated that these markers co-localized, and increased in parallel with fibrosis stage (Fig 4e, $p < 0.03$). The canals of Hering, the most proximal part of the intrahepatic biliary tree, are thought to provide a niche for liver epithelial progenitors, raising the possibility that the hepatic content of Hh responsive progenitors might be influenced by the level of portal inflammation [5]. To address this issue we correlated numbers of K7/Gli2-double (+) cells with the level of portal inflammation. Portal inflammatory activity correlated significantly with the hepatic content of Hh-responsive epithelial progenitors (Fig 4f, $p < 0.03$). Because ballooned hepatocytes are a rich source of Hh ligands and predict fibrosis stage in NAFLD, and progenitor accumulation correlates with fibrosis stage in NAFLD, we next examined the relationship between hepatocyte ballooning and numbers of Hh-responsive progenitors. Numbers of K7/Gli2-double positive cells (Fig 4g), as well as total K7 positive cells, were strongly positively associated with the severity of hepatocyte ballooning ($p < 0.004$ and $p < 0.03$, respectively).

Finally, because expansion of myofibroblastic populations is a hallmark of liver fibrogenesis and tends to parallel accumulation of immature liver epithelial cells in NAFLD [3], Hedgehog-mediated epithelial-to-mesenchymal transition [14], and fibrogenic repair [3], we evaluated the relationship between fibrosis stage and the hepatic content of stromal cells that expressed myofibroblast markers and Gli2. Sections from 27 NAFLD patients with different stages of liver fibrosis were stained for either α -SMA (n=15) or vimentin (n= 12). As expected, patients with advanced fibrosis (S3-4) had greater numbers of α -SMA positive cells than those with less advanced fibrosis (S0-2) (Fig 5a, $p < 0.004$). Similar results were noted when vimentin-stained sections were examined (Fig 5b, $p < 0.002$). Review of slides that were co-stained for vimentin and Gli2 revealed that the stromal cell populations

harbored Hh-responsive (Gli2-positive) cells (Fig 5c) and demonstrated that numbers of Gli2 positive cells and vimentin expression were strongly correlated ($p < 0.003$, ordinal logistic regression, likelihood ratio test).

Clinical correlates of liver fibrosis significantly correlate with hepatic Shh and/or Gli2 staining

Tissue samples in the NASH CRN repository are linked to relevant clinical information, providing a unique opportunity to assess relationships between clinical parameters and liver histology. Therefore, we performed univariate and multivariate analysis to identify clinical correlates (predictors) of liver fibrosis in our study cohort, and then assessed the relationship between these parameters and hepatic Hh pathway activity. Univariate analysis demonstrated significant correlations of fibrosis stage with age, BMI, waist circumference, log HOMA-IR, and HTN (Table 2). All of these variables correlated strongly with hepatic expression levels of Shh (Table 2), which (as noted earlier) significantly correlated with hepatic accumulation of Gli2-positive cells ($p < 0.0001$). Log HOMA-IR correlated with Shh expression even after adjusting for fibrosis stage (cumulative odds ratio (COR) [95% CI] = 3.1 [1.5, 6.9], $p < 0.003$). Similarly, age, BMI, waist circumference, log HOMA-IR, and HTN were significantly correlated with Gli2 expression (Table 3). After adjusting for Shh expression, only hypertension was significantly correlated with Gli2 expression, suggesting that the presence of hypertension was independently associated with higher Gli2 expression at a given Shh ligand level (Table 3).

DISCUSSION

This cross-sectional immunohistochemical analysis of liver biopsies from a large number of well-characterized patients with NAFLD provides compelling evidence that the severity of liver damage (i.e., hepatocyte ballooning, portal inflammation and liver fibrosis) parallels the level of Hh pathway activity in this disease. Genetic and pharmacologic approaches that modulate Hh signaling in experimental animals and liver cell culture models have proven that the Hh pathway regulates several key aspects of liver repair, including the out-growth of liver progenitor populations [12], hepatic recruitment of inflammatory cells [5], generation and accumulation of liver myofibroblasts [4, 13], and fibrogenesis [3]. In animal models of liver injury, transient Hh pathway activation is required for liver regeneration [15], but sustained/excessive Hh signaling promotes cirrhosis [3]. Thus, although direct proof that deregulated Hh signaling mediates NAFLD progression in humans is lacking, the results of the present study demonstrate that this is likely to be true and thus, identify novel diagnostic and therapeutic targets to improve NAFLD outcomes.

Although cross sectional, our data strongly suggest that inter-individual differences in the ability to control Hh pathway activity may contribute to the variable outcomes of fatty liver injury. Our univariate analysis supports this concept by identifying strong correlations between hepatic levels of Shh ligand production or nuclear accumulation of the Hh-regulated transcription factor, Gli2, and each of the three clinical variables that have been most consistently linked with advanced liver fibrosis in NAFLD, i.e., older age, overweight/obesity, and the diagnosis of insulin resistance/type 2 diabetes. Hepatic production of Shh ligands and/or Hh signaling activity were also demonstrated to correlate with other clinical factors that associated with liver fibrosis, including waist circumference and HTN, suggesting a relationship between overly-exuberant Hh pathway activation in the liver and extra-hepatic adverse outcomes of the metabolic syndrome. The aggregate data, therefore, suggest that deregulated Hh pathway activity might promote, and/or result from, the metabolic syndrome, and mediate damage to the liver and other tissues that occurs in this condition. Extension of this logic justifies development of non-invasive tests that quantify

Hh pathway activity in order to identify individuals who are experiencing tissue damage related to the metabolic syndrome before irreparable end-organ damage ensues. Such patients could then be enrolled into prospective clinical trials designed to determine if decreasing Hh pathway activity restores normal tissue repair and prevents (or reverts) progressive tissue damage.

To our knowledge, our study is the first to demonstrate an unequivocal relationship between Hh pathway activity at the tissue level and the severity of damage in that tissue in people with the metabolic syndrome. While novel, evidence that deregulated Hh signaling occurs in the metabolic syndrome and is likely to be directly responsible for related tissue pathology is buttressed by data that were previously reported by our group and others. First, obesity is strongly associated with the metabolic syndrome, and it has been proven that the Hh pathway is a major, highly-conserved, regulator of fat mass [16]. Pathway activation arrests adipogenesis and promotes the accumulation of adipocyte precursors [17]. Mature fat cells themselves are also capable of producing and releasing Hh ligands, and ligand generation from adipose depots is increased in obesity [16]. Moreover, interaction of a key adipocyte-derived anorexogenic hormone, leptin, with its receptors on target cells induces Hh ligand production and activates Hh signaling which, in turn, directly mediates the effects of leptin in those cells [18]. Second, the metabolic syndrome is a chronic inflammatory state, and the Hh pathway is known to have immunomodulatory functions [19]. Hh is required for normal thymic development and regulates the viability, tissue localization, and cytokine production of lymphocytes in adults [20]. In rodents and humans with NASH, for example, hepatic accumulation of pro-fibrogenic natural killer T (NKT) cells correlates with the level of Hh pathway activity and tissue expression of the NKT cell chemoattractant, CXCL16, a Hh-inducible gene. The NKT cells, in turn, likely play a key role in fibrosis progression because in the rodents, NASH-related cirrhosis is prevented by NKT cell depletion. Conversely, livers removed from patients undergoing liver transplantation for NAFLD-related cirrhosis are dramatically enriched with NKT cells [9]. Third, endothelial cell dysfunction/vascular remodeling is a characteristic of the metabolic syndrome, and the Hh pathway is an acknowledged regulator of vasculogenesis/angiogenesis [21]. Membranous microparticles released from cells that produce Hh ligands (e.g., apoptotic T cells and liver cells) contain biologically active Hh ligands that interact with Hh receptors on vascular endothelial cells and initiate Hh signaling [22]. The latter induces endothelial cell activation and alters production of vaso-active substances, such as nitric oxide [23]. Such findings have prompted speculation that Hh signaling is fundamentally involved in the pathogenesis of endothelial cell dysfunction [24]. Fourth, obesity and the metabolic syndrome are known to increase the risk of cancer in various tissues [25]. Hh ligands promote the viability and growth of many types of stem/progenitor cells [26], and deregulated Hh signaling is well-documented in several obesity-associated cancers, including hepatocellular carcinoma [27], which has become one of the main causes of cancer-related death in obese American men [28]. Thus, the cumulative evidence strongly supports the concept that deregulated Hh signaling is broadly relevant to the pathophysiology of the metabolic syndrome. The liver is both a target of, and a contributor to, metabolic syndrome-related pathophysiology, and the present study suggests that both aspects of the relationship are likely to involve the Hh pathway. Additional research is needed to examine this issue, and to determine if plasma levels of Shh identify NAFLD subjects with liver injury who have increased fibrogenesis, and/or if treatments that “normalize” Hh pathway activation would improve recovery from NAFLD.

Acknowledgments

Source of funding The Nonalcoholic Steatohepatitis Clinical Research Network (NASH CRN) is supported by the National Institute of Diabetes and Digestive and Kidney Diseases (NIDDK) (grants U01DK061718,

U01DK061728, U01DK061731, U01DK061732, U01DK061734, U01DK061737, U01DK061738, U01DK061730, U01DK061713), and the National Institute of Child Health and Human Development (NICHD).

Several clinical centers use support from General Clinical Research Centers or Clinical and Translational Science Awards in conduct of NASH CRN Studies (grants UL1RR024989, M01RR000750, M01RR00188, UL1RR02413101, M01RR000827, UL1RR02501401, M01RR000065, M01RR020359, UL1RR025741).

Dr. Manal Abdelmalek is supported by a NIH/NIDDK K23 Career Development Award (K23-DK062116). The analyses described in this study were supported by NIH/NIDDK Grant (PI: Diehl; R01-DK053792 and R01-DK077794) and discretionary funds from the Duke University Division of Gastroenterology.

List of Abbreviations

α-SMA	alpha-smooth muscle actin
CI	confidence interval
COR	cumulative odds ratio
ER	endoplasmic reticulum
G	histologic grade
Gli-2	glioblastoma 2 transcription factor
Hh	hedgehog
HOMA-IR	homeostatic model assessment of insulin resistance
HPF	high power field
K7	keratin 7
MCD	methionine choline-deficient
mRNA	messenger RNA
NAFL	nonalcoholic fatty liver
NAFLD	nonalcoholic fatty liver disease
NASH	nonalcoholic steatohepatitis
NASH CRN	NASH Clinical Research Network
S	fibrosis stage
Shh	sonic Hedgehog
SH	steatohepatitis

REFERENCES

1. Farrell GC, Larter CZ. Nonalcoholic fatty liver disease: from steatosis to cirrhosis. *Hepatology*. 2006; 43:S99–S112. [PubMed: 16447287]
2. Larter CZ, Yeh MM, Haigh WG, Williams J, Brown S, Bell-Anderson KS, Lee SP, et al. Hepatic free fatty acids accumulate in experimental steatohepatitis: role of adaptive pathways. *J Hepatol*. 2008; 48:638–647. [PubMed: 18280001]
3. Syn WK, Jung Y, Omenetti A, Abdelmalek M, Guy CD, Yang L, Wang J, et al. Hedgehog-mediated epithelial-to-mesenchymal transition and fibrogenic repair in nonalcoholic fatty liver disease. *Gastroenterology*. 2009; 137:1478–1488. e1478. [PubMed: 19577569]
4. Choi SS, Omenetti A, Witek RP, Moylan CA, Syn WK, Jung Y, Yang L, et al. Hedgehog pathway activation and epithelial-to-mesenchymal transitions during myofibroblastic transformation of rat hepatic cells in culture and cirrhosis. *Am J Physiol Gastrointest Liver Physiol*. 2009; 297:G1093–1106. [PubMed: 19815628]

5. Omenetti A, Syn WK, Jung Y, Francis H, Porrello A, Witek RP, Choi SS, et al. Repair-related activation of hedgehog signaling promotes cholangiocyte chemokine production. *Hepatology*. 2009; 50:518–527. [PubMed: 19575365]
6. Neuschwander-Tetri BA, Clark JM, Bass NM, Van Natta ML, Unalp-Arida A, Tonascia J, et al. Clinical, Laboratory and Histologic Associations in Adults with Nonalcoholic Fatty Liver Disease. *Hepatology*. 2010; 52:913–924. [PubMed: 20648476]
7. Kleiner DE, Brunt EM, Van Natta M, Behling C, Contos MJ, Cummings OW, Ferrell LD, et al. Design and validation of a histological scoring system for nonalcoholic fatty liver disease. *Hepatology*. 2005; 41:1313–1321. [PubMed: 15915461]
8. Jung Y, McCall SJ, Li YX, Diehl AM. Bile ductules and stromal cells express hedgehog ligands and/or hedgehog target genes in primary biliary cirrhosis. *Hepatology*. 2007; 45:1091–1096. [PubMed: 17464985]
9. Syn WK, Oo YH, Pereira TA, Karaca GF, Jung Y, Omenetti A, Witek RP, et al. Accumulation of natural killer T cells in progressive nonalcoholic fatty liver disease. *Hepatology*. 2010; 51:1998–2007. [PubMed: 20512988]
10. Rangwala F, Guy CD, Lu J, Suzuki A, Burchette JL, Abdelmalek MF, Chen W, Diehl AM. Increased Production of Sonic Hedgehog by Ballooned Hepatocytes. *Journal of Pathology*. 2011 In Press.
11. Omenetti A, Choi S, Michelotti G, Diehl AM. Hedgehog signaling in the liver. *J Hepatol*. 2011; 54:366–373. [PubMed: 21093090]
12. Sicklick JK, Li YX, Melhem A, Schmelzer E, Zdanowicz M, Huang J, Caballero M, et al. Hedgehog signaling maintains resident hepatic progenitors throughout life. *Am J Physiol Gastrointest Liver Physiol*. 2006; 290:G859–870. [PubMed: 16322088]
13. Choi SS, Witek RP, Yang L, Omenetti A, Syn WK, Moylan CA, Jung Y, et al. Activation of Rac1 promotes hedgehog-mediated acquisition of the myofibroblastic phenotype in rat and human hepatic stellate cells. *Hepatology*. 2010; 52:278–290. [PubMed: 20578145]
14. Omenetti A, Porrello A, Jung Y, Yang L, Popov Y, Choi SS, Witek RP, et al. Hedgehog signaling regulates epithelial-mesenchymal transition during biliary fibrosis in rodents and humans. *J Clin Invest*. 2008; 118:3331–3342. [PubMed: 18802480]
15. Ochoa B, Syn WK, Delgado I, Karaca GF, Jung Y, Wang J, Zubiaga AM, et al. Hedgehog signaling is critical for normal liver regeneration after partial hepatectomy in mice. *Hepatology*. 2010; 51:1712–1723. [PubMed: 20432255]
16. Pospisilik JA, Schramek D, Schnidar H, Cronin SJ, Nehme NT, Zhang X, Knauf C, et al. Drosophila genome-wide obesity screen reveals hedgehog as a determinant of brown versus white adipose cell fate. *Cell*. 2010; 140:148–160. [PubMed: 20074523]
17. Suh JM, Gao X, McKay J, McKay R, Salo Z, Graff JM. Hedgehog signaling plays a conserved role in inhibiting fat formation. *Cell Metab*. 2006; 3:25–34. [PubMed: 16399502]
18. Choi SS, Syn WK, Karaca GF, Omenetti A, Moylan CA, Witek RP, Agboola KM, et al. Leptin promotes the myofibroblastic phenotype in hepatic stellate cells by activating the hedgehog pathway. *J Biol Chem*. 2010; 285:36551–36560. [PubMed: 20843817]
19. Uhmman A, Dittmann K, Nitzki F, Dressel R, Koleva M, Frommhold A, Zibat A, et al. The Hedgehog receptor Patched controls lymphoid lineage commitment. *Blood*. 2007; 110:1814–1823. [PubMed: 17536012]
20. Shah DK, Hager-Theodorides AL, Outram SV, Ross SE, Varas A, Crompton T. Reduced thymocyte development in sonic hedgehog knockout embryos. *J Immunol*. 2004; 172:2296–2306. [PubMed: 14764698]
21. Astorga J, Carlsson P. Hedgehog induction of murine vasculogenesis is mediated by Foxf1 and Bmp4. *Development*. 2007; 134:3753–3761. [PubMed: 17881493]
22. Witek RP, Yang L, Liu R, Jung Y, Omenetti A, Syn WK, Choi SS, et al. Liver cell-derived microparticles activate hedgehog signaling and alter gene expression in hepatic endothelial cells. *Gastroenterology*. 2009; 136:320–330. e322. [PubMed: 19013163]
23. Agouni A, Mostefai HA, Porro C, Carusio N, Favre J, Richard V, Henrion D, et al. Sonic hedgehog carried by microparticles corrects endothelial injury through nitric oxide release. *FASEB J*. 2007; 21:2735–2741. [PubMed: 17428963]

24. Meziani F, Tesse A, Andriantsitohaina R. Microparticles are vectors of paradoxical information in vascular cells including the endothelium: role in health and diseases. *Pharmacol Rep.* 2008; 60:75–84. [PubMed: 18276988]
25. Calle EE, Rodriguez C, Walker-Thurmond K, Thun MJ. Overweight, Obesity, and Mortality from Cancer in a Prospectively Studied Cohort of U.S. Adults. *N Engl J Med.* 2003; 348:1625–1638. [PubMed: 12711737]
26. Rangwala F, Omenetti A, Diehl AM. Cancer Stem Cells: Repair Gone Awry? *J Oncol.* 2011; 2011:465343. Epub 2010 Dec 5. [PubMed: 21188169]
27. Sicklick JK, Li Y, Jayaraman A, Kannangai R, Qi Y, Vivekanadan A, Ludlow JW, et al. Dysregulation of the Hedgehog pathway in human hepatocarcinogenesis. *Carcinogenesis.* 2006; 27:748–757. [PubMed: 16339184]
28. Starley BQ, Calcagno CJ, Harrison SA. Nonalcoholic fatty liver disease and hepatocellular carcinoma: a weighty connection. *Hepatology.* 2010; 51:1820–32. [PubMed: 20432259]

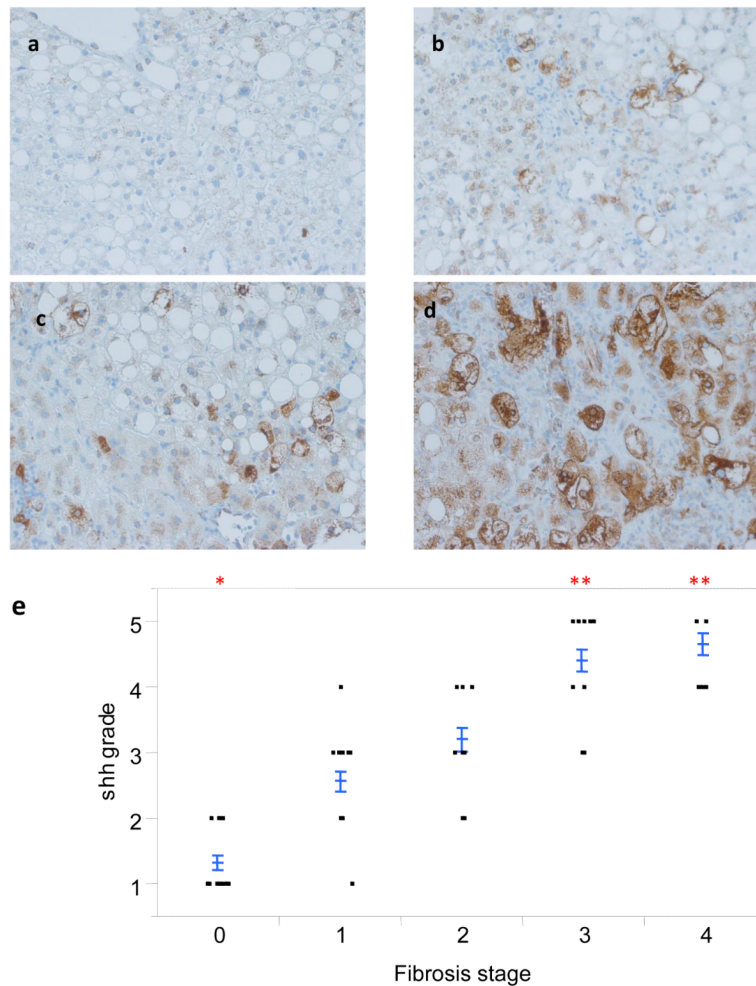


Figure 1. Shh expression correlates with fibrosis stage in NAFLD

Photomicrographs of Shh immunohistochemistry in patients with S0 (a), S2 (b), S3 (c) and S4 (d) fibrosis show increased numbers of positive cells with increased fibrosis stage (x400 magnification). The immunohistochemistry scoring results were semi-quantified into 5 ranks and the results were plotted according to the fibrosis stage as scored by the NASH CRN Pathology Committee using trichrome-stained liver sections (e). Closed circles represent individual subjects. The bold line represents the mean value, while whiskers with horizontal lines (upper and lower) represent the standard error. $p < 0.0001$ (Kruskal-Wallis test). $p < 0.005$ (α -level adjusted for 10 post-hoc comparison pairs): * (vs. stage 1 and 2) and ** (vs. stage 0, 1, and 2).

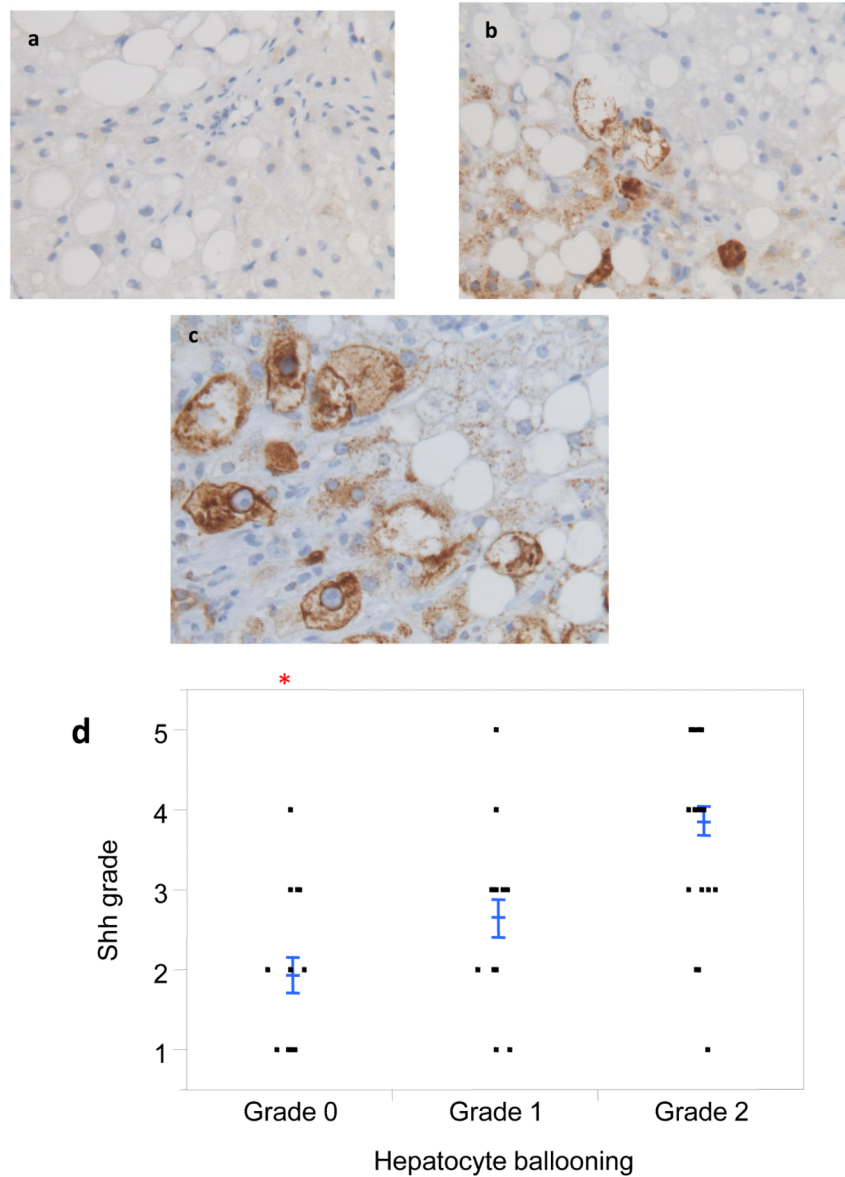


Figure 2. Shh expression correlates with hepatocyte ballooning

Photomicrographs of Shh immunohistochemistry in patients with Grade 0 (a), Grade 1 (b), and Grade 2 (c) ballooning show increased numbers of positive cells with increased ballooning grade (x400 magnification). Shh expression was plotted relative to the grade of hepatocyte ballooning as scored by the NASH CRN Pathology Committee using H&E-stained liver sections (d). Closed circles represent individual subjects. The bold line represents the mean value, while whiskers with horizontal lines (upper and lower) represent the standard error. $p < 0.0001$ (Kruskal-Wallis test); * $p < 0.017$ vs. grade 1 and 2 (α -level adjusted for 3 post-hoc comparison pairs).

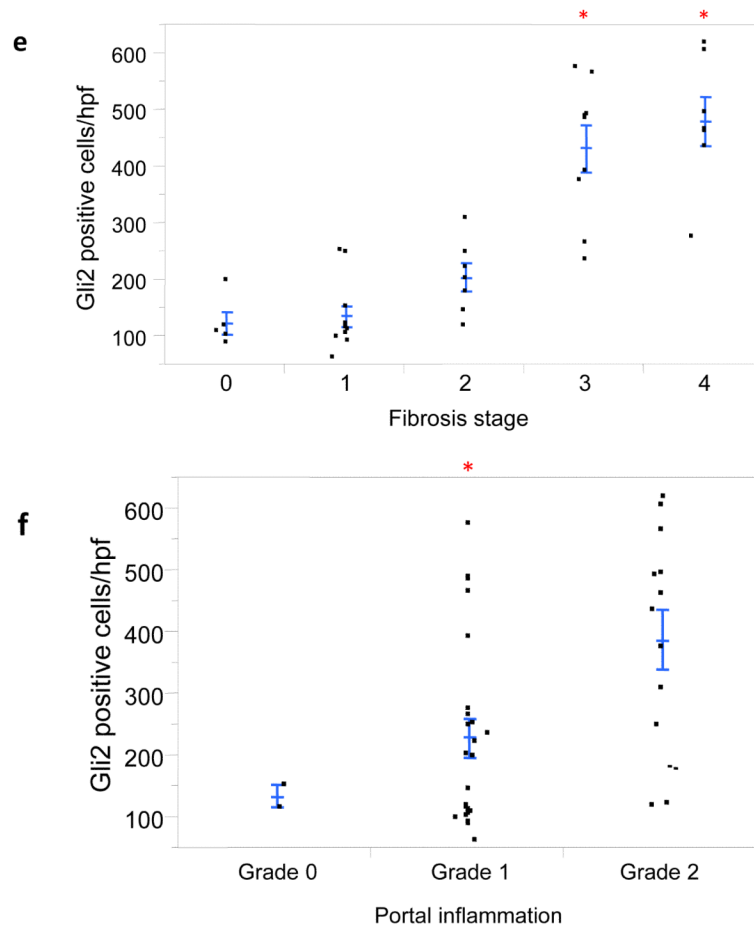
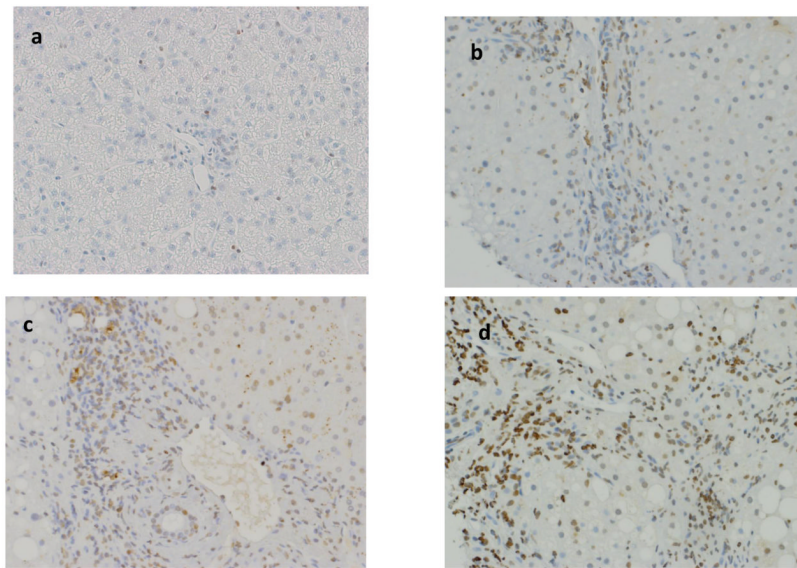


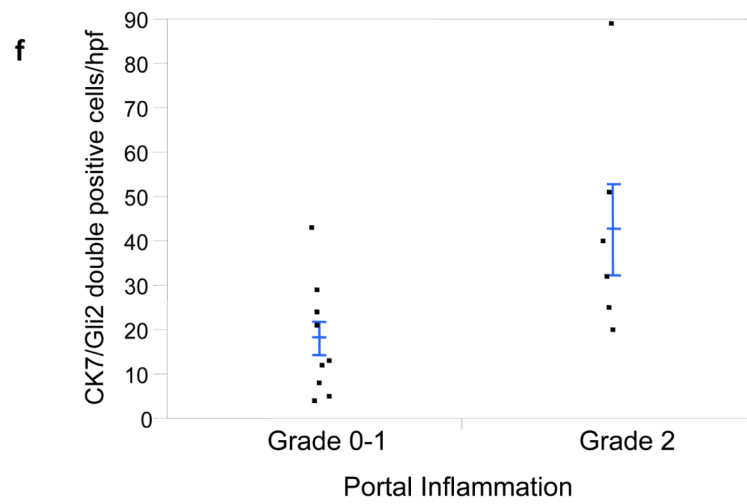
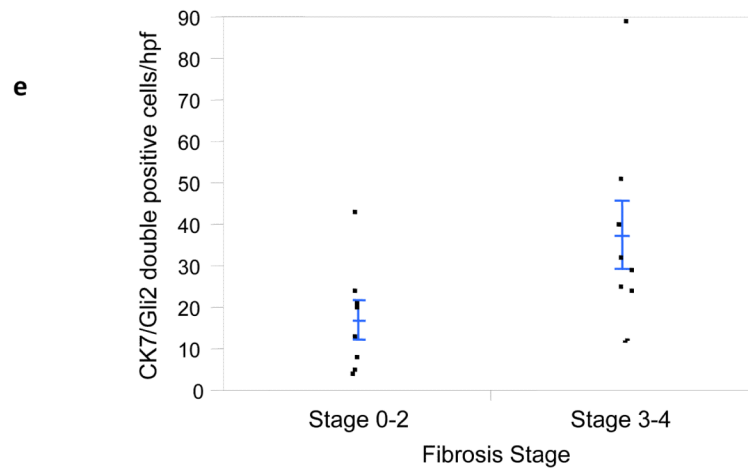
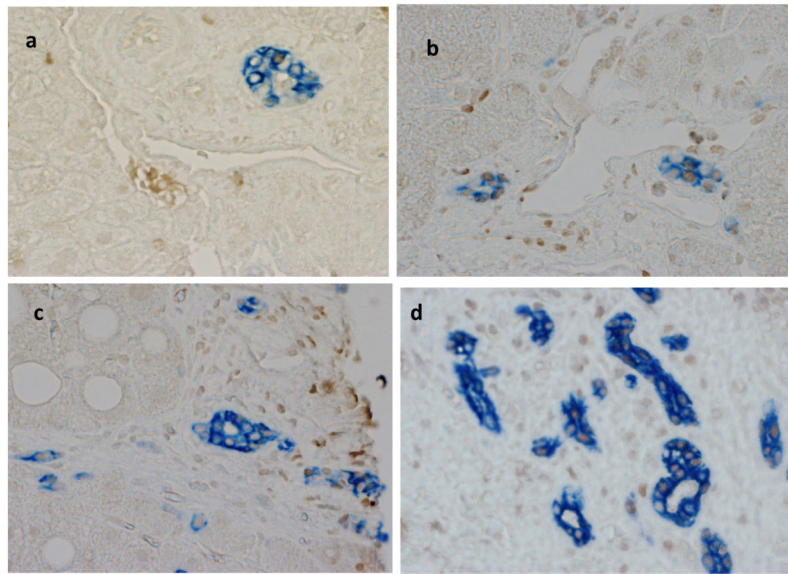
Figure 3. Numbers of Gli2+ cells correlate with fibrosis stage and grade of portal inflammation
 Photomicrographs of Gli2 immunohistochemistry in patients with S0 (a), S2 (b), S3 (c), and S4 (d) fibrosis show increased numbers of positive cells (nuclear staining) with increased fibrosis stage (x400 magnification). The Gli2 staining scores were plotted relative to fibrosis

stage (**e**), as well as portal inflammation grade (**f**). Closed circles represent individual subjects. The bold line represents the mean value, while whiskers with horizontal lines (upper and lower) represent the standard error. Significant stage/grade-related differences are shown, * $p < 0.005$ (vs. stage 0, 1, and 2) (**e**) and * $p < 0.017$ vs. grade 2 (α -level adjusted for 10 and 3 post-hoc comparison pairs for fibrosis stage and portal inflammation grade, respectively).

\$watermark-text

\$watermark-text

\$watermark-text



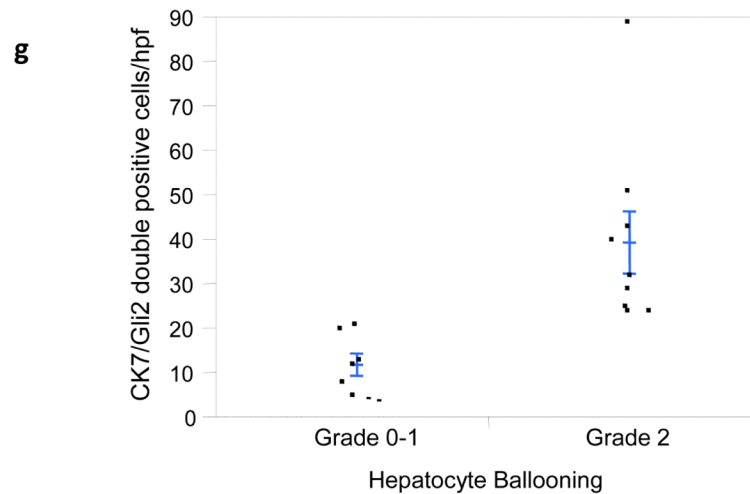


Figure 4. Hepatic accumulation of liver progenitor cells increases with fibrosis stage, portal inflammation, and hepatocyte ballooning in NAFLD

Photomicrographs of liver sections double-stained for keratin 7 (blue) and Gli2 (brown) in patients with S0 (a), S2 (b), S3 (c) and S4 (d) fibrosis show increased numbers of positive cells with increased fibrosis stage (x400 magnification). Keratin 7-positive cells and Gli2-positive cells were counted in double-stained liver biopsy sections. The average cell counts (per x400 HPF) were plotted in relationship to fibrosis (e), portal inflammation (f), and hepatocyte ballooning (g). In each graph, closed circles represent individual subjects. The bold line represents the mean value while whiskers with horizontal lines (upper and lower) represent standard error. $p < 0.05$, 0.03, and 0.004 for fibrosis, portal inflammation, and ballooning, respectively (Kruskal-Wallis test).

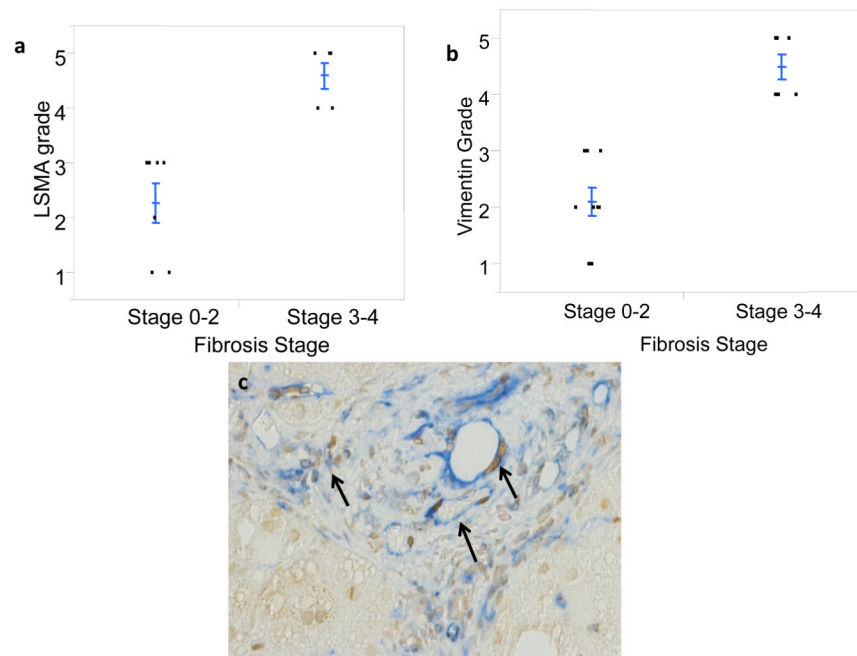


Figure 5. Numbers of myofibroblastic cells increase with fibrosis stage

Liver biopsies were stained with α -SMA or vimentin to identify myofibroblastic mesenchymal cells. The liver content of α -SMA positive cells (LSMA) (a) or vimentin-stained cells (b) were quantified as described in the Methods and correlated with fibrosis stage based on NASH CRN Pathology Committee review of trichrome-stained sections. Closed circles represent individual subjects. The bold line represents the mean value while whiskers with horizontal lines (upper and lower) represent standard error. LSMA grade and vimentin grade were higher in livers with advanced fibrosis, $p < 0.004$ and $p < 0.002$, respectively. (c) The photomicrograph illustrates accumulation of Hh-responsive mesenchymal cells in fibrotic NAFLD. Arrows demonstrate stromal-vascular cells in fibrotic septa double-stained for vimentin (blue) and Gli2 (brown).

TABLE 1

Clinical Characteristics of the study population

N=90	Summary Statistics
Age (years)	48 ± 13
Female gender, %	59
Hispanic, %	14
Race, % White; Asian/Pacific islanders; Others	81; 7; 12
BMI (kg/m ²)	35 ± 7
Type II Diabetes mellitus, %	30
Hypertension, %	46
Hyperlipidemia, %	56
Steatosis grade, % G0; G1; G2; G3	4; 37; 33; 26
Lobular inflammation grade, % G0; G1; G2; G3	0; 56; 38; 6
Ballooning grade, % G0; G1; G2	26; 31; 43
Portal inflammation grade, % G0; G1; G2	11; 62; 27
Fibrosis stage, % S0; S1; S2; S3; S4	26; 25; 16; 22; 11

TABLE 2

Associations of clinical variables with fibrosis stage and Shh expression

	Fibrosis stage	Shh expression
	COR and 95% CI	COR and 95% CI
Age, 5 units change	1.3[1.1, 1.5] (p<0.0008)	1.3[1.1, 1.5] (p<0.005)
BMI, 5 units change	1.6[1.2, 2.2] (p<0.001)	1.6[1.2, 2.1] (p<0.002)
Waist circumference, 5 units change	1.3[1.1, 1.5] (p<0.0006)	1.3[1.1, 1.5] (p<0.0007)
Log (HOMA-IR)	2.5[1.4, 4.5] (p<0.002)	3.4[1.8, 6.4] (p<0.0001)
Diabetes mellitus	2.1[0.9, 4.9] (p=0.08)	2.8[1.2, 6.5] (p<0.02)
Hypertension	3.1[1.4, 6.9] (p=0.005)	2.6[1.2, 5.7] (p<0.02)

COR: cumulative odds ratio computed in ordinal logistic regression models using fibrosis stage or shh expression score as an outcome variable. CI: confidence interval.

TABLE 3

Associations of clinical variables with Gli2 expression

	Unadjusted	Adjusted*
	$\beta \pm SE$	$\beta \pm SE$
Age, 1 units change	4.1 \pm 2.1 (p=0.006)	3.0 \pm 2.0 (p=0.145)
BMI, 1 units change	11.0 \pm 4.1 (p=0.011)	5.0 \pm 3.5 (p=0.169)
Waist circumference, 5 units change	4.2 \pm 1.9 (p=0.04)	0.7 \pm 1.7 (p=0.656)
Log (HOMA-IR)	97.1 \pm 41.3 (p=0.024)	-21.9 \pm 41.1 (p=0.597)
Diabetes mellitus	90.9 \pm 61.0 (p=0.145)	8.8 \pm 42.3 (p=0.854)
Hypertension	181.3 \pm 48.5 (p=0.0006)	123.8 \pm 39.1 (p=0.0034)

* adjusted for Shh expression levels, β : beta coefficient computed in linear regression models using Gli2 expression (cell numbers per HPF) as an outcome variable.